

**NATIONAL ADVISORY COMMITTEE  
FOR AERONAUTICS**

---

**REPORT No. 644**

**THE TORSIONAL AND BENDING DEFLECTION OF  
FULL-SCALE ALUMINUM-ALLOY PROPELLER BLADES  
UNDER NORMAL OPERATING CONDITIONS**

By **EDWIN P. HARTMAN** and **DAVID BIERMANN**



**1938**

## AERONAUTIC SYMBOLS

### 1. FUNDAMENTAL AND DERIVED UNITS

	Symbol	Metric		English	
		Unit	Abbreviation	Unit	Abbreviation
Length.....	$l$	meter.....	m	foot (or mile).....	ft. (or mi.)
Time.....	$t$	second.....	s	second (or hour).....	sec. (or hr.)
Force.....	$F$	weight of 1 kilogram.....	kg	weight of 1 pound.....	lb.
Power.....	$P$	horsepower (metric).....		horsepower.....	hp.
Speed.....	$V$	{kilometers per hour.....	k.p.h.	miles per hour.....	m.p.h.
		{meters per second.....	m.p.s.	feet per second.....	f.p.s.

### 2. GENERAL SYMBOLS

<p><math>W</math>, Weight=<math>mg</math></p> <p><math>g</math>, Standard acceleration of gravity=<math>9.80665</math> m/s<sup>2</sup> or 32.1740 ft./sec.<sup>2</sup></p> <p><math>m</math>, Mass=<math>\frac{W}{g}</math></p> <p><math>I</math>, Moment of inertia=<math>mk^2</math>. (Indicate axis of radius of gyration <math>k</math> by proper subscript.)</p> <p><math>u</math>, Coefficient of viscosity</p>	<p><math>\nu</math>, Kinematic viscosity</p> <p><math>\rho</math>, Density (mass per unit volume)</p> <p>Standard density of dry air, 0.12497 kg-m<sup>-4</sup>-s<sup>2</sup> at 15° C. and 760 mm; or 0.002378 lb.-ft.<sup>-4</sup> sec.<sup>2</sup></p> <p>Specific weight of "standard" air, 1.2255 kg/m<sup>3</sup> or 0.07651 lb./cu. ft.</p>
---	--

### 3. AERODYNAMIC SYMBOLS

<p><math>S</math>, Area</p> <p><math>S_w</math>, Area of wing</p> <p><math>G</math>, Gap</p> <p><math>b</math>, Span</p> <p><math>c</math>, Chord</p> <p><math>b^2</math>, Aspect ratio</p> <p><math>\bar{S}</math>, True air speed</p> <p><math>V</math>, Dynamic pressure=<math>\frac{1}{2}\rho V^2</math></p> <p><math>q</math>, Lift, absolute coefficient <math>C_L = \frac{L}{qS}</math></p> <p><math>D</math>, Drag, absolute coefficient <math>C_D = \frac{D}{qS}</math></p> <p><math>D_0</math>, Profile drag, absolute coefficient <math>C_{D_0} = \frac{D_0}{qS}</math></p> <p><math>D_i</math>, Induced drag, absolute coefficient <math>C_{D_i} = \frac{D_i}{qS}</math></p> <p><math>D_p</math>, Parasite drag, absolute coefficient <math>C_{D_p} = \frac{D_p}{qS}</math></p> <p><math>C</math>, Cross-wind force, absolute coefficient <math>C_C = \frac{C}{qS}</math></p> <p><math>R</math>, Resultant force</p>	<p><math>i_w</math>, Angle of setting of wings (relative to thrust line)</p> <p><math>i_s</math>, Angle of stabilizer setting (relative to thrust line)</p> <p><math>Q</math>, Resultant moment</p> <p><math>\Omega</math>, Resultant angular velocity</p> <p><math>\rho \frac{Vl}{\mu}</math>, Reynolds Number, where <math>l</math> is a linear dimension (e.g., for a model airfoil 3 in. chord, 100 m.p.h. normal pressure at 15° C., the corresponding number is 234,000; or for a model of 10 cm chord, 40 m.p.s., the corresponding number is 274,000)</p> <p><math>C_p</math>, Center-of-pressure coefficient (ratio of distance of c.p. from leading edge to chord length)</p> <p><math>\alpha</math>, Angle of attack</p> <p><math>\epsilon</math>, Angle of downwash</p> <p><math>\alpha_0</math>, Angle of attack, infinite aspect ratio</p> <p><math>\alpha_i</math>, Angle of attack, induced</p> <p><math>\alpha_a</math>, Angle of attack, absolute (measured from zero-lift position)</p> <p><math>\gamma</math>, Flight-path angle</p>
--	--

---

---

**REPORT No. 644**

---

**THE TORSIONAL AND BENDING DEFLECTION OF  
FULL-SCALE ALUMINUM-ALLOY PROPELLER BLADES  
UNDER NORMAL OPERATING CONDITIONS**

By **EDWIN P. HARTMAN** and **DAVID BIERMANN**  
Langley Memorial Aeronautical Laboratory

---

---

I

## NATIONAL ADVISORY COMMITTEE FOR AERONAUTICS

HEADQUARTERS, NAVY BUILDING, WASHINGTON, D. C.  
LABORATORIES, LANGLEY FIELD, VA.

Created by act of Congress approved March 3, 1915, for the supervision and direction of the scientific study of the problems of flight (U. S. Code, Title 50, Sec. 151). Its membership was increased to 15 by act approved March 2, 1929. The members are appointed by the President, and serve as such without compensation.

JOSEPH S. AMES, Ph. D., *Chairman*,  
Baltimore, Md.

DAVID W. TAYLOR, D. Eng., *Vice Chairman*,  
Washington, D. C.

WILLIS RAY GREGG, Sc. D., *Chairman, Executive Committee*,  
Chief, United States Weather Bureau.

WILLIAM P. MACCRACKEN, J. D., *Vice Chairman, Executive Committee*,  
Washington, D. C.

CHARLES G. ABBOT, Sc. D.,  
Secretary, Smithsonian Institution.

LYMAN J. BRIGGS, Ph. D.,  
Director, National Bureau of Standards.

ARTHUR B. COOK, Rear Admiral, United States Navy,  
Chief, Bureau of Aeronautics, Navy Department.

HARRY F. GUGGENHEIM, M. A.,  
Port Washington, Long Island, N. Y.

SYDNEY M. KRAUS, Captain, United States Navy,  
Bureau of Aeronautics, Navy Department.

CHARLES A. LINDBERGH, LL. D.,  
New York City.

DENIS MULLIGAN, J. S. D.,  
Director of Air Commerce, Department of Commerce.

AUGUSTINE W. ROBINS, Brigadier General, United States  
Army,

Chief Matériel Division, Air Corps, Wright Field,  
Dayton, Ohio.

EDWARD P. WARNER, Sc. D.,  
Greenwich, Conn.

OSCAR WESTOVER, Major General, United States Army,  
Chief of Air Corps, War Department.

ORVILLE WRIGHT, Sc. D.,  
Dayton, Ohio.

---

GEORGE W. LEWIS, *Director of Aeronautical Research*

JOHN F. VICTORY, *Secretary*

HENRY J. E. REID, *Engineer-in-Charge, Langley Memorial Aeronautical Laboratory, Langley Field, Va.*

JOHN J. IDE, *Technical Assistant in Europe, Paris, France*

---

### TECHNICAL COMMITTEES

AERODYNAMICS  
POWER PLANTS FOR AIRCRAFT  
AIRCRAFT MATERIALS

AIRCRAFT STRUCTURES  
AIRCRAFT ACCIDENTS  
INVENTIONS AND DESIGNS

*Coordination of Research Needs of Military and Civil Aviation*

*Preparation of Research Programs*

*Allocation of Problems*

*Prevention of Duplication*

*Consideration of Inventions*

LANGLEY MEMORIAL AERONAUTICAL LABORATORY

LANGLEY FIELD, VA.

Unified conduct, for all agencies, of  
scientific research on the fundamental  
problems of flight.

OFFICE OF AERONAUTICAL INTELLIGENCE

WASHINGTON, D. C.

Collection, classification, compilation,  
and dissemination of scientific and tech-  
nical information on aeronautics.

## REPORT No. 644

# THE TORSIONAL AND BENDING DEFLECTION OF FULL-SCALE ALUMINUM-ALLOY PROPELLER BLADES UNDER NORMAL OPERATING CONDITIONS

By EDWIN P. HARTMAN and DAVID BIERMANN

### SUMMARY

*The torsional deflection of the blades of three full-scale aluminum-alloy propellers operating under various loading conditions was measured by a light-beam method. Angular bending deflections were also obtained as an incidental part of the study.*

*The deflection measurements showed that the usual present-day type of propeller blades twisted but a negligible amount under ordinary flight conditions. A maximum deflection of about  $\frac{1}{10}^\circ$  was found at a  $V/nD$  of 0.3 and a smaller deflection at higher values of  $V/nD$  for the station at 0.70 radius. These deflections are much smaller than would be expected from earlier tests, but the light-beam method is considered to be much more accurate than the direct-reading transit method used in the previous tests.*

### INTRODUCTION

In propeller research and design it would often be highly desirable to know just how much a propeller blade twists under operating conditions. For example, in a recent research project carried out at the N. A. C. A. for the purpose of determining the effect of compressibility on the performance of propellers in the take-off and climbing range (reference 1), a shifting of the basic propeller-coefficient curves with varying tip speed was found. The magnitude and direction of the shift was such that it could be explained either as a result of compressibility of the air or as an effect of a twisting deflection of the propeller blades. Obviously it is desirable to separate these two effects; and the only convenient method of doing so is to measure the actual deflection of the blades under various loading conditions.

Similar displacements of propeller-coefficient curves were encountered in certain propeller tests (reference 2) made at the California Institute of Technology. In that case the torsional deflection of the blades under load was given as a plausible explanation of a shifting of the thrust-coefficient and efficiency curves with increasing tip speeds and power inputs.

From considerations of propeller design and selection, it is desirable to know the extent of the torsional deflection of propeller blades under load, for upon this knowledge depends the magnitude of the correction factor to be applied in the selection of a propeller to absorb a given engine power. Weick gives some arbitrary

values of blade deflection to be used in connection with the design charts of reference 3. These values amount to a  $\frac{1}{2}^\circ$  increase in blade angle at  $0.75R$  for each increment of 100 horsepower above 200 horsepower and are assumed to apply only for horsepowers of 500 or less.

The instances cited give a good indication of the need for blade-deflection data. The present measurements on current types of aluminum-alloy propellers should therefore be of value.

Contemporaneously with the present tests, a series of blade-deflection measurements (reference 4) was made at Wright Field. These measurements, which covered

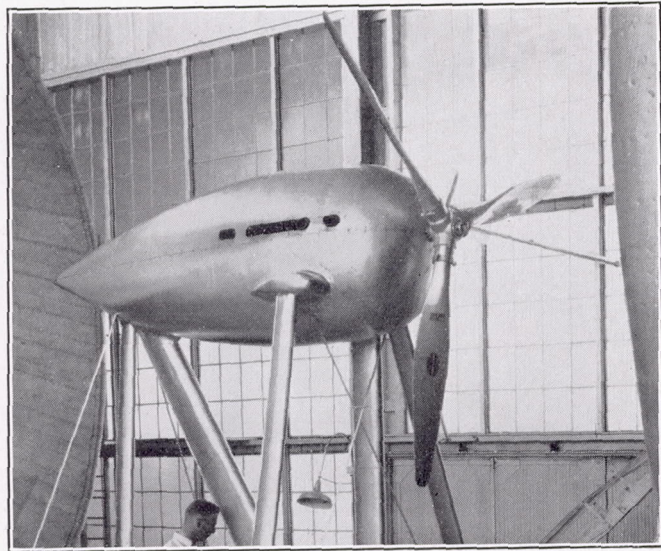


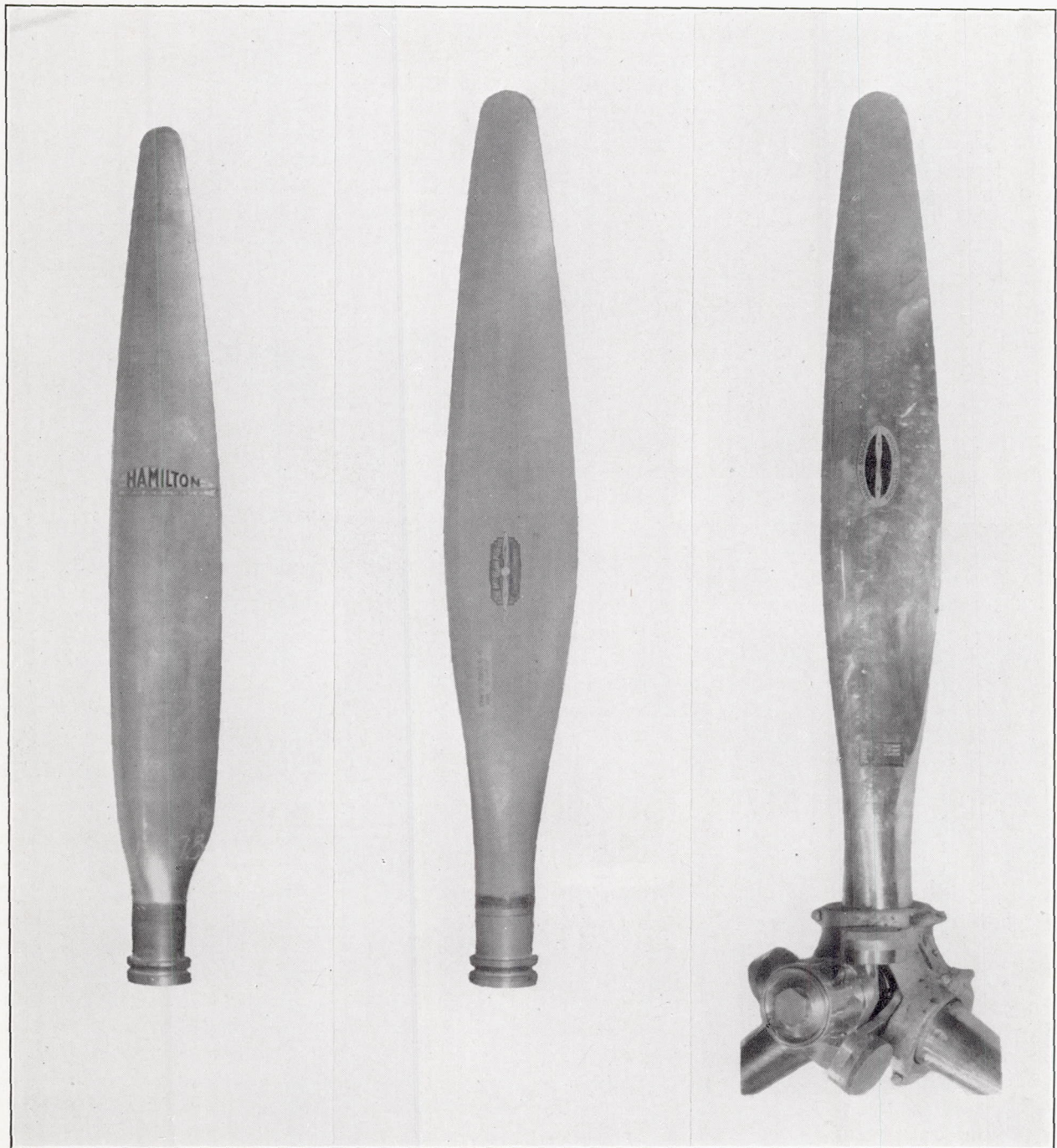
FIGURE 1.—Test set-up showing engine nacelle and propeller.

a large range of revolution speeds and a series of stations along the blade, showed torsional blade deflections of sufficient magnitude to account for a large part of the shift in the coefficient curves caused by increasing the tip speed. Unfortunately, the measurements were only for static ( $V/nD=0$ ) conditions. The method used at Wright Field for making deflection measurements is similar to one that was employed by the N. A. C. A. to obtain the deflection data published in reference 5. It depends on transit measurements of the distance between the leading and the trailing edges of a particular section measured parallel to the propeller axis. The angle of twist is calculated from the changes in this distance that occur when the propeller is operating.

The light-beam method of measuring blade deflection employed in the present investigation is believed to be of much greater accuracy than the transit method. A comparison of the results obtained in this report with those obtained for the same propeller by the transit method (reference 4) shows large differences. The transit method is known to be subject to a number of possible errors. Perhaps the greatest source of error lies in the fact that either torsional or bending vibrations will tend to make the measured distance between the leading and trailing edges of the section, and there-

fore the apparent blade angle, greater than it actually is. The torsional blade deflection computed from these measured distances is likely to be much too large on this account.

The angular deflection of the blade in forward bending was also measured in the present tests. The bending deflection of propeller blades probably has a negligible aerodynamic effect though it has some significance in structural design. In the present tests, it was obtained directly as a part of the light-beam method without any special modifications.



4877

5868-9

6101

FIGURE 2.—Propeller blades tested.

The light-beam method of measuring blade deflections will probably be used in the future, perhaps for other purposes than measuring blade deflection, as it offers possibilities for use in measuring flutter and vibration frequencies of propeller blades. It is a modification of a method used by the British for the deflection measurements reported in reference 6.

TEST EQUIPMENT AND PROPELLERS

The deflection measurements were made in the N. A. C. A. 20-foot tunnel described in reference 7. The tunnel has an open throat and its maximum air speed is about 110 miles per hour.

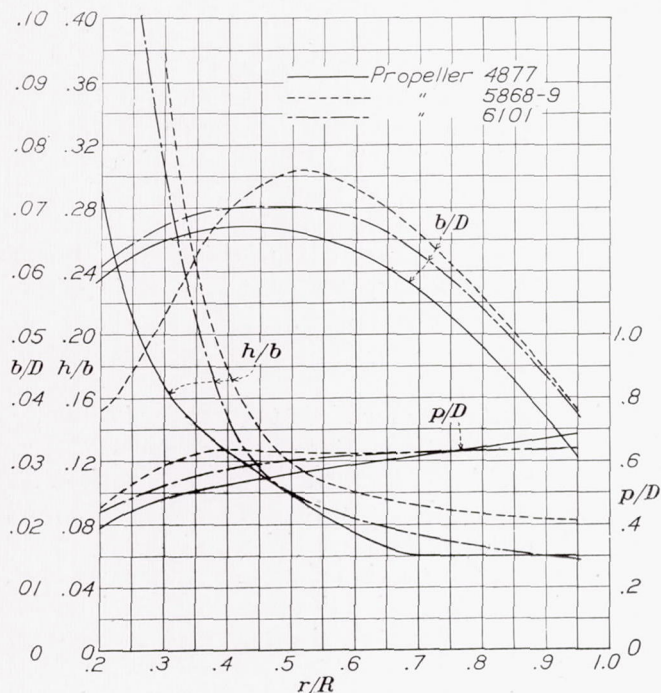


FIGURE 3.—Blade-form curves for propellers 4877, 5868-9, and 6101. Blade angle, 15° at 0.75R. D, diameter; R, radius to the tip; r, station radius; h, section thickness; b, section chord; p, geometric pitch.

The propellers were turned by a 600-horsepower Curtiss Conqueror engine enclosed in a liquid-cooled engine nacelle. The engine-propeller set-up, shown in figure 1, had previously been used for standard propeller tests. A complete description of it is given in reference 8.

Deflection measurements were made of three aluminum-alloy propellers of Clark Y section further identified as follows:

Design drawing No.	Number of blades	Diameter (ft.)	Blade thickness at 0.75R (h/b)
Navy 5868-9	2	10	9
Hamilton Standard 6101	3	10	7
Navy 4877	2	9½	6

A photograph of the three blade types is shown in figure 2 and the blade-form curves are given in figure 3.

DEFLECTION-MEASURING APPARATUS AND METHODS

General method.—A small plane mirror was cemented to the face of the propeller blade at the station at which measurements were to be made. With the blade in a horizontal position an intense pencil of light was directed onto the mirror, which reflected it to a focus on a vertical screen behind the propeller. As the propeller rotated, the narrow pencil of light impinged on the mirror for only a small fraction of each revolution, thus having the effect of a stroboscope. Bending and

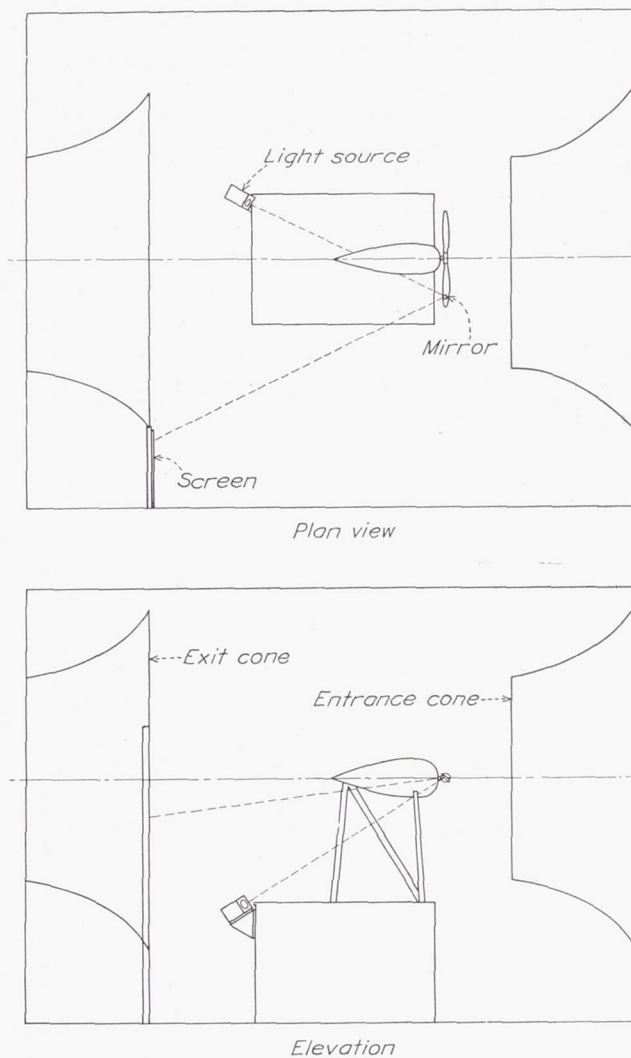


FIGURE 4.—Diagram of set-up.

torsional deflections caused the image on the screen to move horizontally and vertically, respectively, through angular displacements easily calculated when the distance from the mirror to the screen is known. In the present tests this distance was great enough to make very accurate readings possible. The testing was done in the dark. A diagrammatic sketch of the apparatus mounted in the test chamber is shown in figure 4.

**Light unit.**—The light unit consisted of a wooden projection box with a 6–8 volt straight-filament automobile lamp and a high-quality  $f$  6.0 lens of 20-inch focal length taken from an aerial camera. The lamp was supplied with current from a storage battery and the lens holder was adjustable for focusing.

**Mirror.**—The mirror was  $\frac{1}{2}$  inch square and  $\frac{1}{4}$  inch thick. It was cemented to the flat face of the propeller blade with melted Canada balsam. When the mirror was carefully attached, it showed little tendency to fly off.

**Screen.**—The plywood screen was attached rigidly to the tunnel framework at one side of the exit cone. (See fig. 4.) The records were obtained by an observer who marked the position of the reflected light spot on a large sheet of white paper temporarily attached to the screen. A level reference line was put on each record before it was removed. This line was parallel to a horizontal line passing through the mirror and the propeller-shaft center.

**Image.**—The lens system was adjusted until a sharp image of the filament (with propeller stopped) was found on the screen. During operation, the intensity of the reflected spot is reduced in the ratio of the mirror width to the circumference of the circle that the mirror describes. This reduction in light intensity necessitates testing in the dark.

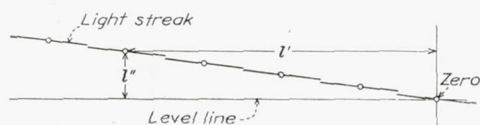


FIGURE 5.—Diagram showing appearance of the records taken.

As the incident pencil of light was of finite width, the mirror was illuminated through a small but appreciable portion of the circle it described around the propeller axis. The mirror, during its passage through the light pencil, also rotated in space through a small arc around an axis passing through the mirror and normal to the propeller disk. This motion was sufficient to cause the image to move and to produce a short streak of light on the screen. The direction of the streak was nearly the same as the direction of movement of the image resulting from a bending deflection. Since the end points of the streak were a little indefinite, the bending deflection measurements are somewhat less accurate than the torsional-deflection measurements. The light bulb was so orientated that the image of the straight filament lay parallel to the streak caused by the mirror sweeping through the pencil of light. All measurements were made to the midpoint of the recorded streak. The resulting records for various loading conditions (different r. p. m.) looked very much like the diagram in figure 5. In this figure  $l'$  represents the bending deflection for a given loading condition and  $l''$  represents the torsional deflection. As the source of light was fixed, the angles subtended at the

mirror by the distances  $l'$  and  $l''$  were just twice the actual angles of bending and twist.

**Calibration.**—In actual operation the motion of the image caused by bending was not quite horizontal (parallel to the blade) nor was the motion caused by twisting the blade quite vertical. Correction factors for the small deviations of the motions of the image from the horizontal and vertical due to pure bending and pure twisting were obtained by calibrating the twist and bending against the motion of the image on the screen. For the calibration, the bending deflections were obtained by means of a wire and turnbuckle attached to the end of the blade. Twisting deflections were obtained by turning the blade in the hub and using an inclinometer to measure the blade angles.

#### ACCURACY

It is estimated that the angles of twist are within  $\frac{1}{20}^\circ$  of being correct and that the angle of forward bending is within  $\frac{1}{10}^\circ$ . Transit observations of the engine mounting indicated no appreciable angular motion of the engine. The errors introduced by movements of the screen due to the deflection of the tunnel wall to which it was attached are known to be within the specified limits of accuracy.

#### THEORY OF BLADE DEFLECTION

An important cause for blade twist under load is the air force acting at the center of pressure of each section. The position of the center of pressure varies with angle of attack (which is an inverse function of  $V/nD$ ) and may, under certain conditions, be considerably displaced from the elastic axis of the propeller blade. The position of the elastic axis along the chord is shown in reference 9 to be approximately at the center of gravity of the area produced by plotting the cube of the thickness against the chord. For a Clark Y section, 10 percent thick, the elastic axis will lie at about 39 percent of the chord back from the leading edge. The elastic axis will move backward as the thickness decreases and forward as the thickness increases.

The greatest twisting effect due to air forces will probably occur at high, unstalled angles of attack (low values of  $V/nD$ ) where the air forces are relatively high and where the center of pressure has moved to its maximum forward position (about 30 percent of the chord from the leading edge at air speeds below the compressibility burble). As  $V/nD$  increases, the air forces become less and the center of pressure moves toward the trailing edge, thus reducing the positive (i. e., tending to increase the blade angle) twisting deflections. At high values of  $V/nD$  near zero thrust, the center of pressure moves to the other side of the elastic axis, but the air forces are so small that negative deflections of any considerable magnitude due to this cause are unlikely to occur. The deflections due to air forces may thus be considered as essentially positive throughout the normal take-off and flight range.

The quantitative effect of the centrifugal forces on blade deflection is a little uncertain. There will be a general tendency for each small element of mass throughout the blade ( $dm$ , fig. 6) to remove itself as far as possible from the center of rotation. In figure 6 it is seen that the distance of the elemental mass  $dm$  from the axis of rotation becomes greater as the blade angle approaches zero. It appears, then, that the component of centrifugal force acting parallel to the  $x$  axis (fig. 6) tends to decrease the blade angle. The component acting parallel to the  $z$  axis tends to do just the opposite. Its action, which may be more effective than that of the  $x$  component, tends to remove the natural twist from the blade in the same manner that a twisted strip of tin will untwist under a tensile end load. The effect of the  $z$  component is thus to increase the blade angle, and the net deflection caused by centrifugal forces will be positive or negative depending upon which component predominates.

It should also be mentioned that forward rake (or forward bending deflections) will materially change the torsional deflection caused by centrifugal forces. Inasmuch as the air forces on the blade produce forward bending, it is clear that a variation in air load alone will result in a change of the torsional deflection caused by centrifugal forces. This fact makes more difficult the separation of the torsional deflections caused by centrifugal and air forces.

### RESULTS AND DISCUSSION

The results of the blade-deflection measurements for the three propellers tested are shown in figures 7 to 13. The following table shows the test conditions and the various figures in which the results are plotted:

Figure	Propeller	Blade angle at $0.75R$ (deg.)	Stations at which measurements were made ( $r/R$ )
7 and 8.....	5868-9	15	0.70
9.....	5868-9	15	.85
10.....	5868-9	20	.70
11.....	6101	15	.70
12 and 13.....	4877	15	.70

The data are presented in two different forms of chart: In one, the propeller rotation speed was held constant while the  $V/nD$  was varied; and in the other, the  $V/nD$  was held approximately constant at the lowest value obtainable and the propeller rotational speed was varied. The first type of chart is the most instructive, but the second type shows the various rotational speeds at which flutter occurs. (See fig. 13.)

The most important fact indicated by the figures is that the twisting deflections of the blades are very small, almost negligible, which is contrary to generally accepted ideas about blade deflection and quite different from the results of previous tests.

The largest deflections measured were for propeller 4877 (figs. 12 and 13) which, even in the important part

of the take-off range, amounted to only  $\frac{1}{4}^\circ$ . This propeller has a blade-thickness ratio at  $0.75R$  of only 6 percent of the chord and its thickness ratio throughout its full radius is considerably less than for most of the propellers in use today.

The deflection at  $0.70R$  for propellers 5868-9 and 6101, which are typical of present-day propellers, amounted to about  $\frac{1}{10}^\circ$  in the most important part of the take-off range and less for other ranges of flight operation. Such deflections could not account for any large part of the shift in the curves of basic propeller coefficients with increasing tip speeds. Any shifting

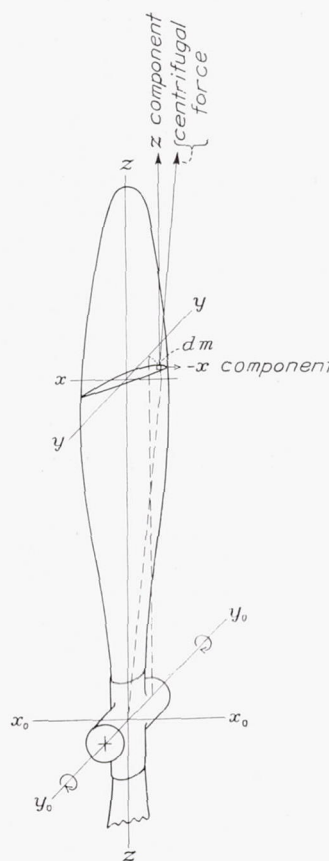


FIGURE 6.—Diagram illustrating the way that centrifugal force tends to change the blade angle.

effect of this sort must therefore be considered as resulting from causes other than blade deflection. Furthermore, in the selection of a propeller diameter and a blade angle to absorb a given power, it will usually be quite unnecessary to make any allowance for the blade deflections of present-day aluminum-alloy propellers.

In the range of  $V/nD$  values between zero and the value for zero thrust, there is a point where the effective torsional deflection caused by air forces will be zero. It was estimated that this point would be at a  $V/nD$  of about 0.6 for a blade set  $15^\circ$  at  $0.75R$ . At this value of  $V/nD$  in figures 7, 9, 11, and 12, the torsional deflections should be largely the result of centrifugal forces.

It will be observed that in all cases the torsional deflections at a  $V/nD$  of 0.6 are very small and, in all but one case (propeller 6101, fig. 11), they are positive. From this observation it appears that, for the blades tested, the  $z$  components of the centrifugal forces, which tend to increase the blade angle, were, in general, more powerful than the  $x$  components, which tend to decrease the blade angle.

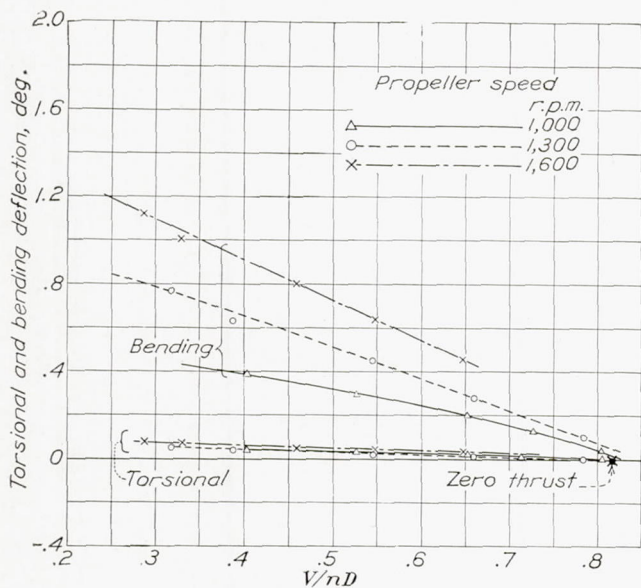


FIGURE 7.—Blade deflections at 0.70R for propeller 5868-9 set 15° at 0.75R.

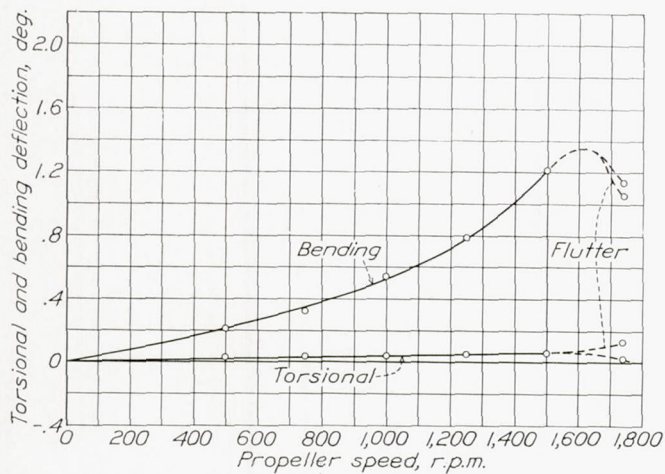


FIGURE 8.—Blade deflections at 0.70R for propeller 5868-9 set 15° at 0.75R.  $V/nD$ , approximately 0.23.

The fluttering tendencies of propeller 4877 are illustrated in figure 13. It was noted that the flutter became more severe with increasing rotational speeds and decreasing  $V/nD$  values. When fluttering, the propeller emitted a sound similar to that usually associated with supersonic tip speeds and the thrust and torque were considerably affected, as indicated in reference 1. It was noticed on certain occasions when the propeller was fluttering that a double image was found on the screen. On other occasions three or more

distinct images were found. The multiple images are easily explained by the fact that the system acts as a stroboscope and the beam of light catches the propeller in a different phase of the vibrational movement on each succeeding revolution. The maximum distance between images will not necessarily be the full amplitude of the vibration but, as the number of separate images increases, the full amplitude is more nearly

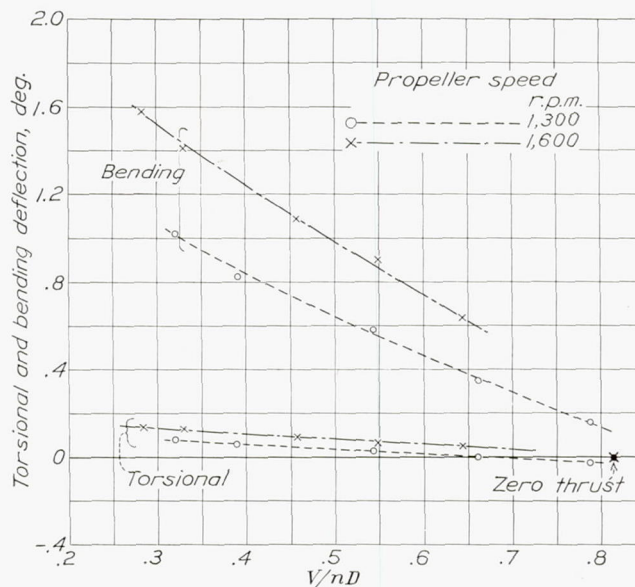


FIGURE 9.—Blade deflections at 0.85R for propeller 5868-9 set 15° at 0.75R.

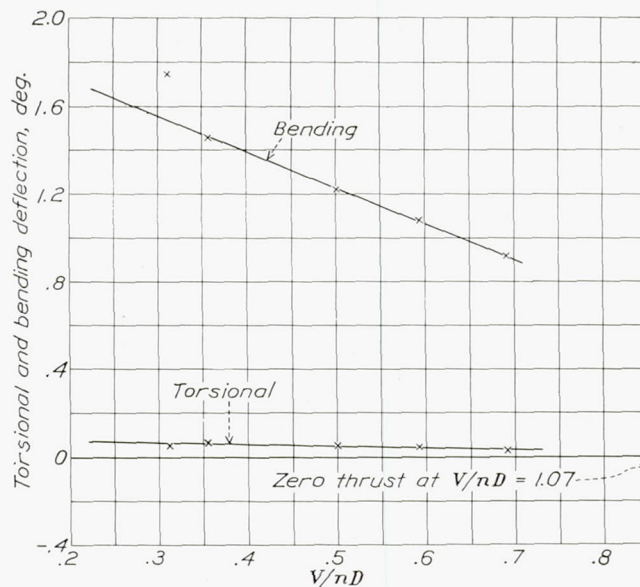


FIGURE 10.—Blade deflections at 0.70R for propeller 5868-9 set 20° at 0.75R. Propeller speed, 1,500 r. p. m.

approached. In figure 13 the plotted points represent the maximum distance between the separate images. The vibrational frequency of the blades should be a simple, though possibly indeterminate, function of the number of images and the rotational speed.

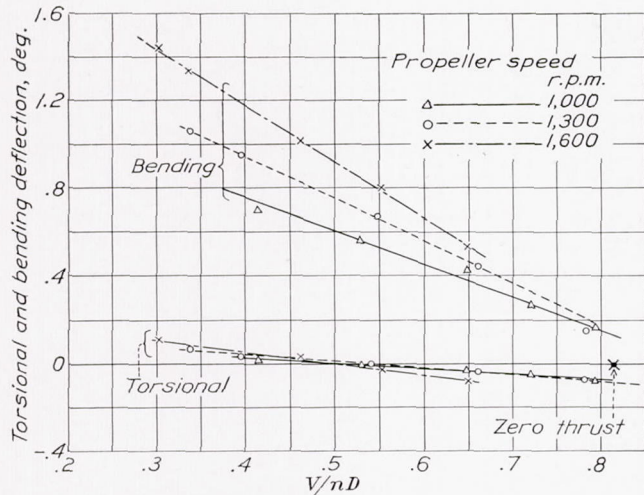


FIGURE 11.—Blade deflections at 0.70R for propeller 6101 set 15° at 0.75R.

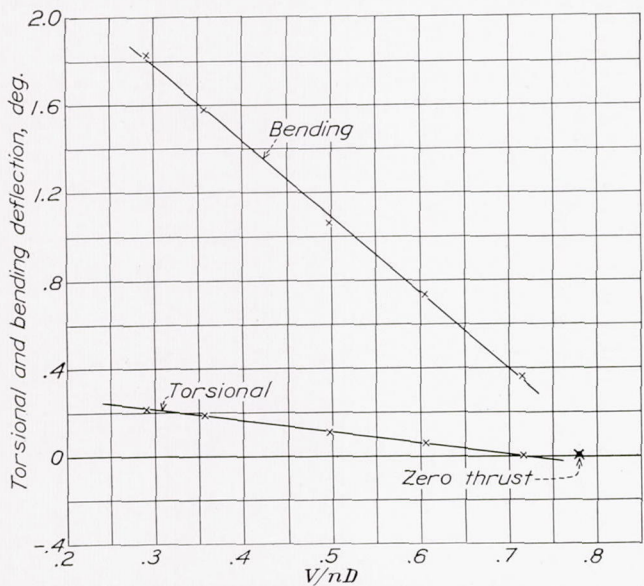


FIGURE 12.—Blade deflections at 0.70R for propeller 4877 set 15° at 0.75R. Propeller speed, 1,500 r. p. m.

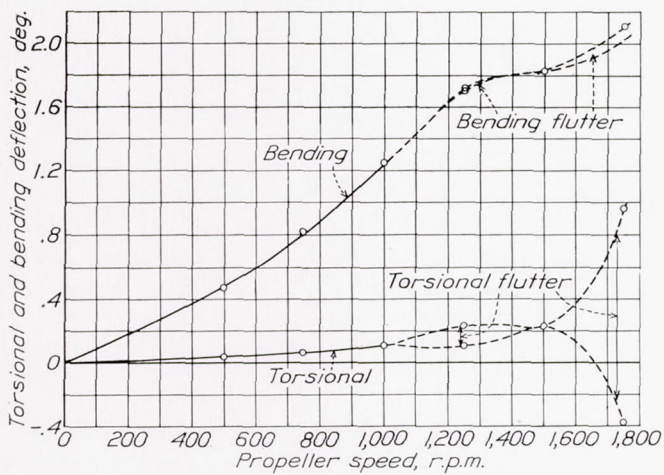


FIGURE 13.—Blade deflections at 0.70R for propeller 4877 set 15° at 0.75R.  $V/nD$ , approximately 0.18.

Propeller 5868-9 fluttered at the tips at high rotational speeds and low values of  $V/nD$ , but the amplitude of the vibration seemed to be small. The marked change in slope of the bending-deflection curve when the blade fluttered (see figs. 8 and 13) is a curious phenomenon that does not seem to be accounted for by a loss in thrust due to flutter for, under these conditions, the thrust actually increases slightly as shown in reference 1.

An examination of figures 7 and 9 indicates that the torsional deflection of a propeller blade probably increases from hub to tip. The two stations tested (0.70R and 0.85R) represent, fairly well, the portion of the blade having the greatest effect on aerodynamic performance.

The maximum torsional deflection for a blade angle of 20° (fig. 10) is very little different from that for a blade angle of 15° (fig. 7). There is probably little advantage in making tests beyond 20° except to determine the effect on blade deflection of blade stall. Since the center of pressure of a stalled blade approaches the elastic axis of the blade, the torsional deflection, caused by air forces, beyond the stall should be less than before the stall occurs, as was mentioned earlier. The torsional deflection caused by the  $x$  component (see fig. 6) of the centrifugal force does, however, depend on the blade-angle setting, which may be justification for testing at high angles.

CONCLUSIONS

1. The measured torsional deflections, in the normal operating range, of two present-day types of aluminum-alloy propellers were almost negligible. One-tenth of a degree or less was measured at the 0.70 radius.
2. The torsional deflection at the 0.85R station was somewhat greater than at the 0.70R station.
3. The light-beam method of measuring blade deflection appears to be a very accurate method of making such measurements and might be of some use in propeller-vibration research.

LANGLEY MEMORIAL AERONAUTICAL LABORATORY,  
 NATIONAL ADVISORY COMMITTEE FOR AERONAUTICS,  
 LANGLEY FIELD, VA., January 18, 1938.

## APPENDIX

## NOTES ON IMPROVEMENT OF METHOD

No time was taken during the present tests to perfect the light-beam method of measuring deflections; however, the tests did reveal certain features of the equipment and method that could be improved. A few suggestions will be given for the benefit of those who wish to use the method in the future.

It is highly desirable to keep the beam of light as narrow as possible throughout its full length since the length of the reflected image (streak of light) on the screen, which should be short for accuracy, depends on the width of the light beam at the mirror. The larger the spot of light at the mirror, the longer is the reflected image and the less accurate is the determination of its midpoint. On the assumption that a certain speed of lens is required, it appears from theory that the smallest diameter lens system having this speed is most desirable. Practically, however, the diameter will probably be limited because of distortion of the image. The optimum diameter, which will depend on the dimensions of the light source, is not known but it is believed to be somewhat less than the  $3\frac{1}{8}$ -inch aperture of the lens used in these tests.

The distance from the mirror to the screen should be great enough to provide good accuracy of reading. In the present tests this distance was about 29 feet, giving approximately 1 foot deflection per degree of twist.

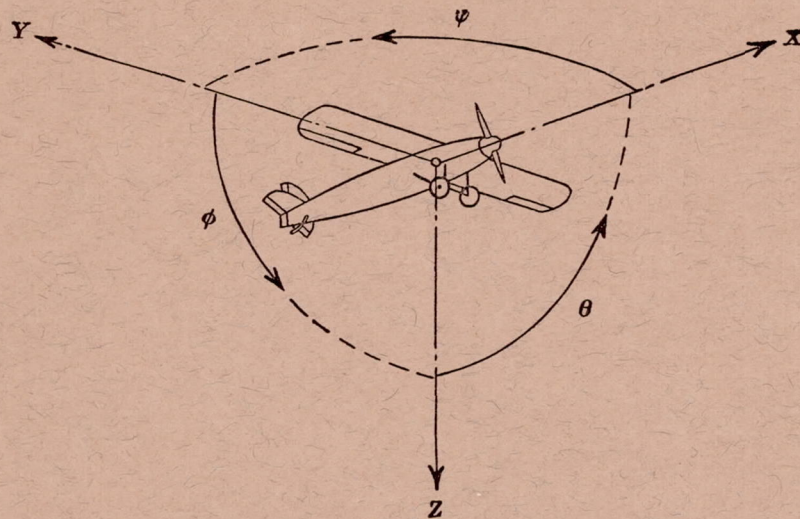
The engine mounting should be rigid enough to prevent angular movements of the engine. Translational movements are not magnified and, if small, have no serious effect.

The angular position of the propeller should be definitely established in the zero position and the light beam then centered on the mirror.

The Canada balsam used to cement the mirrors onto the blades seemed to be satisfactory for the tip speeds encountered in the present tests although a few did fly off under the more severe conditions of tip speed and flutter. It is believed that a firmer adhesive might be desirable, or necessary, for higher tip speeds or very bad flutter conditions. An unsuccessful attempt was made to polish a spot on a blade to mirror smoothness for the purpose of eliminating the attached mirror.

## REFERENCES

1. Biermann, David, and Hartman, Edwin P.: The Effect of Compressibility on Eight Full-Scale Propellers Operating in the Take-Off and Climbing Range. T. R. No. 639 N. A. C. A., 1938.
2. Russell, J. S., and McCoy, H. M.: Wind Tunnel Tests on a High Wing Monoplane with Running Propeller. Part I. Propulsive Characteristics of Two and Three Bladed Adjustable Pitch Propellers Extended to Fairly Large Blade Angles. Jour. Aero. Sci., vol. 3, no. 3, Jan. 1936, pp. 75-76.
3. Weick, Fred E.: Working Charts for the Selection of Aluminum Alloy Propellers of a Standard Form to Operate with Various Aircraft Engines and Bodies. T. R. No. 350, N. A. C. A., 1930.
4. Enos, Louis H.: Some Full Scale Static Propeller Characteristics. Jour. Aero. Sci., vol. 5, no. 1, Nov. 1937, pp. 25-28.
5. Wood, Donald H.: Full-Scale Tests of Metal Propellers at High Tip Speeds. T. R. No. 375, N. A. C. A., 1931.
6. Douglas, G. P., Perring, W. G. A., and Fairthorne, R. A.: Wind Tunnel Tests with High Tip Speed Airscrews. Experimental Investigation of Blade Twist under Load. R. & M. No. 1272, British A. R. C., 1930.
7. Weick, Fred E., and Wood, Donald H.: The Twenty-Foot Propeller Research Tunnel of the National Advisory Committee for Aeronautics. T. R. No. 300, N. A. C. A., 1928.
8. Biermann, David, and Hartman, Edwin P.: Tests of Five Full-Scale Propellers in the Presence of a Radial and a Liquid-Cooled Engine Nacelle, Including Tests of Two Spinners. T. R. No. 642, N. A. C. A., 1938.
9. Wood, R. McKinnon, and Perring, W. G. A.: Stresses and Strains in Airscrews with Particular Reference to Twist. R. & M. No. 1274, British A. R. C., 1930.



Positive directions of axes and angles (forces and moments) are shown by arrows

Axis		Force (parallel to axis) symbol	Moment about axis			Angle		Velocities	
Designation	Sym- bol		Designation	Sym- bol	Positive direction	Designa- tion	Sym- bol	Linear (compo- nent along axis)	Angular
Longitudinal.....	X	X	Rolling.....	L	Y → Z	Roll.....	φ	u	p
Lateral.....	Y	Y	Pitching.....	M	Z → X	Pitch.....	θ	v	q
Normal.....	Z	Z	Yawing.....	N	X → Y	Yaw.....	ψ	w	r

Absolute coefficients of moment

$$C_l = \frac{L}{qbS}$$

(rolling)

$$C_m = \frac{M}{qcS}$$

(pitching)

$$C_n = \frac{N}{qbS}$$

(yawing)

Angle of set of control surface (relative to neutral position),  $\delta$ . (Indicate surface by proper subscript.)

#### 4. PROPELLER SYMBOLS

$D$ , Diameter

$p$ , Geometric pitch

$p/D$ , Pitch ratio

$V'$ , Inflow velocity

$V_s$ , Slipstream velocity

$T$ , Thrust, absolute coefficient  $C_T = \frac{T}{\rho n^2 D^4}$

$Q$ , Torque, absolute coefficient  $C_Q = \frac{Q}{\rho n^2 D^5}$

$P$ , Power, absolute coefficient  $C_P = \frac{P}{\rho n^3 D^5}$

$C_s$ , Speed-power coefficient  $= \sqrt[5]{\frac{\rho V^5}{P n^2}}$

$\eta$ , Efficiency

$n$ , Revolutions per second, r.p.s.

$\Phi$ , Effective helix angle  $= \tan^{-1}\left(\frac{V}{2\pi r n}\right)$

#### 5. NUMERICAL RELATIONS

1 hp. = 76.04 kg-m/s = 550 ft-lb./sec.

1 metric horsepower = 1.0132 hp.

1 m.p.h. = 0.4470 m.p.s.

1 m.p.s. = 2.2369 m.p.h.

1 lb. = 0.4536 kg.

1 kg = 2.2046 lb.

1 mi. = 1,609.35 m = 5,280 ft.

1 m = 3.2808 ft.

